BUBBLE STRUCTURE OF ENAMEL COATINGS AND ITS DETERMINATION

VIKTOR BENEŠ, VÁCLAV BOUŠE[a], MARGARITA SLÁMOVÁ[b], VLADIMÍR SUCHÁNEK[b], KAREL VOLENÍK[c]

Czech Technical University, Faculty of Engineering, Dept of Mathematics, Karlovo nám. 13, 121 35 Praha 2
[a] *SMALT Ltd, 267 62 Komárov u Hořovic*
[b] *Research Institute for Metals, Panenské Břežany, 250 70 Odolena Voda*
[c] *National Research Institute for the Protection of Materials, 190 11 Praha 9 - Běchovice*

Received 16. 7. 1993

The bubble structure of enamel coatings affects their behaviour in corrosion environments and their applicability in the protection of metals against corrosion. A method enabling to characterize the bubble structure of enamel coatings was developed. After preparing a planar section parallel to the coating surface, the diameters of bubble sections are measured, preferably by image analysis. The resulting size distribution of two-dimensional bubble sections can be converted in the size distribution of three-dimensional bubbles using a stereological method. Examples of two different enamel coatings on steel substrate show the applicability of this method to real enamel systems.

INTRODUCTION

Enamel coatings have been widely used for corrosion protection of metals and for decorative purposes. The usual industrial application consists in enamelling of steel or cast iron product.

One of the important properties of enamel coatings is their bubble structure, which develops as a result of gas evolution during firing [1 – 4].

The mechanism of gas evolution is not yet fully understood. However, it is assumed that reactions both in the bulk of enamel melt and at the metal - enamel melt interface contribute to this phenomenon. Gas evolution in the bulk depends mainly on clay content in mill additions. The interface reactions are influenced by the composition of the ambient atmosphere (e.g. by water vapour content) and of the substrate (e.g. by carbon content in steel).

The bubble structure affects the corrosion properties of the coating in two ways:

1. The presence of large bubbles, the diameter of which is comparable to the coating thickness, deteriorates the coating because thin bubble walls are broken easily and the substrate is locally exposed to corrosion environment.
2. On the other hand, uniformly distributed small bubbles are desirable because they reduce the tendency towards "fishscaling".

The bubble size may vary in a wide range. This depends on the substrate and enamel composition and on firing conditions.

Several methods can be used to visualize the bubbles:

a) An X-ray defectoscopic method consisting in taking X-ray photographs of enamel coatings separated from the metallic substrate. During the exposure to transmitted X-rays, the film is in close contact with the separated coating. The separation can be carried out by a chemical method [5] based on dissolution of the steel substrate in an iodine-methanol solution, which is applicable virtually to any inorganic non-metallic coating.

b) Cross-sections of enamel coatings in contact with the substrate can be studied by metallographic techniques.

c) In a similar way, enamel coatings separated from the substrate and mechanically fractured can be investigated.

d) Planar sections parallel to enamel coating surface can be prepared. The distance of such a planar section from the surface can be chosen in advance. The choice is based on the preliminary inspection of a cross-section. It is possible to study one or more planar sections of the same enamel coating, preferably by image analysis complemented by a stereological evaluation.

The X-ray defectoscopic method is practical for comparing differing bubble structures of coatings, however, it is not very suitable for quantitative measurements because of superimposed bubbles and of some uncertainty in bubble image contours definition.

The number of bubbles intersected by a cross-section or by a fracture surface may be too small for a statistical interpretation. The bubble structure within a cross-section or a fracture surface may be inhomogeneous, i.e. it may depend on the distance from the enamel coating surface. If so, this complicates the bubble structure description though, on the other hand, it enables a deeper insight into the mechanism of gas evolution.

A method based on image analysis of planar sections parallel to the surface and on a stereological interpretation of the results appears to be the most effective of the above mentioned methods, in particular in quantitative studies of bubble structure geometry.

PROCEDURE

For obtaining a well-defined planar section of an enamel coating, techniques commonly used in metallography are applicable. The section must be prepared with much care because of high brittleness of enamels. Each planar section parallel to the surface is obtained by removing an adequate layer of enamel by grinding. This must be followed by careful polishing so as to obtain well-defined contours of bubble sections. From the image analysis of a specimen prepared in this way, a sort of bubble size distribution can be obtained. This distribution does not relate to the true bubble diameters but only to the diameters of circles resulting from bubble intersection by an arbitrary plane.

Classical stereological methods are capable of reconstructing the distribution of real spherical bubble diameters and of estimating the volume fraction of bubbles. The application of such a method means a transition from a two-dimensional probe (i.e. a planar section of the coating) to a three-dimensional case (i.e. to a volume in a close neighbourhood of this plane).

The procedure applied in this paper consisted of four steps:

1. Preparation of coating planar sections. An enamel layer, the thickness of which was equal to the preset depth, was removed by wet grinding using papers STRUERS No 220 – 800 followed by polishing with diamond pastes (particle size of 3 μm and 1 μm).

2. Bubble section diameters in the specimen area A were measured by an image analyzer IBAS II. To classify the bubble section diameters, size intervals of constant width were chosen (their number was k). For each (i-th) size interval, the number n_i^* of bubble sections in the whole specimen area was determined.

3. The size distribution of two-dimensional bubble sections was represented in a histogram of n_i versus bubble section diameter values where $n_i = \frac{n_i^*}{A}$ is the number of bubble sections in the i-th interval per unit area.

4. For reconstructing the real three-dimensional distribution of bubbles as a function of the true bubble diameter values, a stereological method (Scheil-Schwartz-Saltykov method) was used. The problem of determining the distribution of spherical bubbles randomly localized in the sample volume as a function of the true bubble diameter is based on the solution of a classical integral equation ([6], p. 289). The most frequent way of determining the required solution is the discretization of the problem. First, the maximum true diameter is set equal to the maximum section diameter. Now the following system of equations is solved ([6], p. 294):

$$n_i = \Delta \sum_{j=1}^{k} b_{ij} N_j \qquad i = 1, 2, \ldots, k$$

Here Δ is the width of the size interval (it is the same for all size intervals), N_j is the unknown number of bubbles in the j-th size interval per unit volume, and b_{ij} is defined as follows:

$$b_{ij} = \sqrt{j^2 - (i-1)^2} - \sqrt{j^2 - i^2} \qquad \text{for } i \leq j;\ j = 1, 2, \ldots, k$$

$$b_{ij} = 0 \qquad \text{for } i > j$$

The solution of this system of equations is

$$N_j = \frac{1}{\Delta} \sum_{i=1}^{k} c_{ij} n_i$$

The coefficients c_{ij} for 1 to 15 size intervals are listed in [7], p. 280. For a larger number of size intervals, the values of c_{ij} must be calculated.

The mean number N_V of spherical bubbles per unit volume can be estimated easily:

$$N_V = \sum_{j=1}^{k} N_j$$

Further, the estimate of the mean diameter α and the mean volume V of a spherical bubble is possible (see [8], equations (4.18) and (4.20)):

$$\alpha = \frac{\Delta}{N_V} \sum_{j=1}^{k} \left(j - \frac{1}{2}\right) N_j$$

$$V = \frac{\pi}{6} \left[\frac{\Delta^3}{N_V} \sum_{j=1}^{k} \left(j - \frac{1}{2}\right)^3 N_j - \frac{\alpha \Delta^2}{4} \right]$$

Finally, the best way of estimating the volume fraction of spherical bubbles in the specimen near the section plane is given by the formula

$$V_V = A_A$$

where A_A is the area fraction of bubble sections in the planar probe.

EXAMPLES OF PROCEDURE APPLICATION

To illustrate the use of the above described procedure in investigating the bubble structure of particular coatings, two ground-coat enamels were chosen. At present time, both are used in enamelling industry.

The enamels were deposited on both sides of a continuously cast steel sheet (standard ČSN 11 310) 1.0 mm thick containing 0.04% C, 0.20% Mn, 0.012% P,

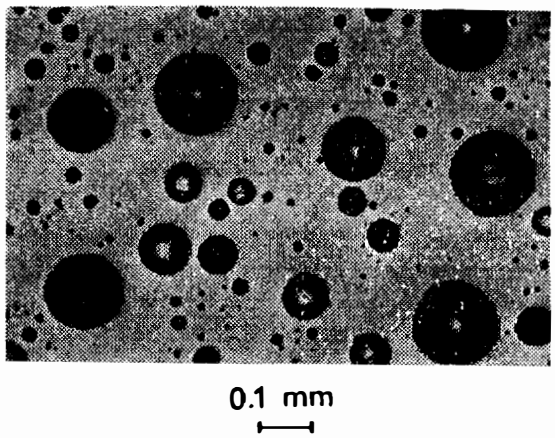

Fig. 1. Optical micrograph of a planar section of enamel coating No 1.

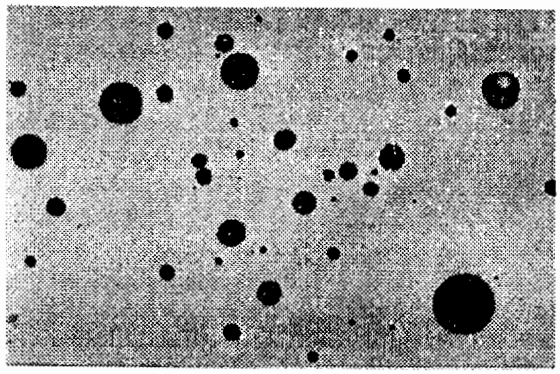

Fig. 2. Optical micrograph of a planar section of enamel coating No 2. For magnification see Fig. 1.

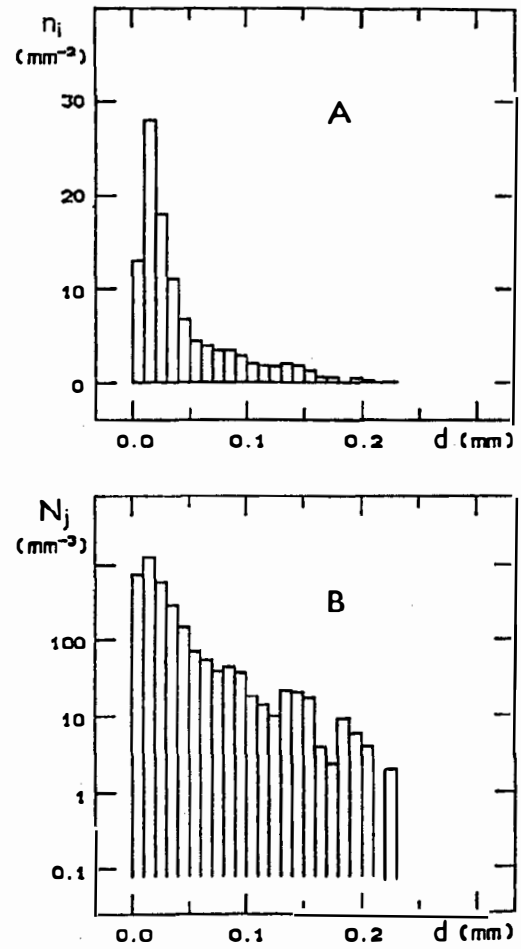

Fig. 3. Size distribution of bubbles, enamel coating No 1. Upper diagram (A): Size distribution of bubble sections determined by image analysis.
Lower diagram (B): Size distribution of three-dimensional bubbles determined by stereological evaluation of image analysis results.
n_i ... *number of bubble sections in the i-th size interval per unit area,*
N_j ... *number of bubbles in the j-th size interval per unit volume,*
α ... *diameter.*

0.011% S, 0.03% Si. The surface was degreased in an organic solvent and pickled in diluted hydrochloric acid before enamelling.

Specification of the enamels:

Enamel No 1:

Conventional ground-coat enamel based on three frits (ZP 10801, ZP 10842, ZP 40841). Mill additions: milled silica, feldspar, clays, bentonite, fluorite, sodium nitrite, water. Firing temperature in the range of 830 – 860°C. The firing temperatures of individual frits are different, which results in inhomogeneous and relatively coarse bubble structure of this enamel.

Enamel No 2:

Low-temperature ground-coat enamel based on three frits (Z 107, Z 111, Z 166). Mill additions: milled silica, clays, borax, bentonite, sodium nitrite, water. The adherence to steel is high even if the firing temperature is as low as 780°C. The bubble structure is fine and homogeneous. Under specified conditions, this enamel can be applied to sheet steel treated merely by degreasing (i.e. pickling or blast cleaning is not required). However, this was not the case in the present work.

Firing parameters:

6.5 minutes; 830°C (enamel No 1), 820°C (enamel No 2).

The cross-sections of both coatings showed that the character of the bubble structure did not change with the distance from the surface. That is why only one planar section parallel to the surface of each coating was studied.

Optical micrographs of planar sections of both enamel coatings are shown in Figs. 1 and 2.

Table 1

Data characterizing the bubble structure of enamel coatings

Coating No	t μm	h μm	α μm	V (10^{-6}mm^3)	V_V	N_V (mm^{-3})	$N_V^{0.1}$ (mm^{-3})
1	200	110	26.3	97	0.296	3420	127
2	150	70	20.6	15	0.013	859	4

Quantitative results obtained from both enamel coatings are given in Figs. 3 and 4. In the upper part of each figure, a histogram obtained by image analysis is shown. The lower parts give the reconstructed bubble size distributions. Semi-logarithmic coordinates are used in the latter diagrams to emphasize large bubbles because as a rule their number is low (in coatings effective in corrosion protection it should be as low as possible). The calculations were carried out for 30 size intervals, the width of each being 10 μm.

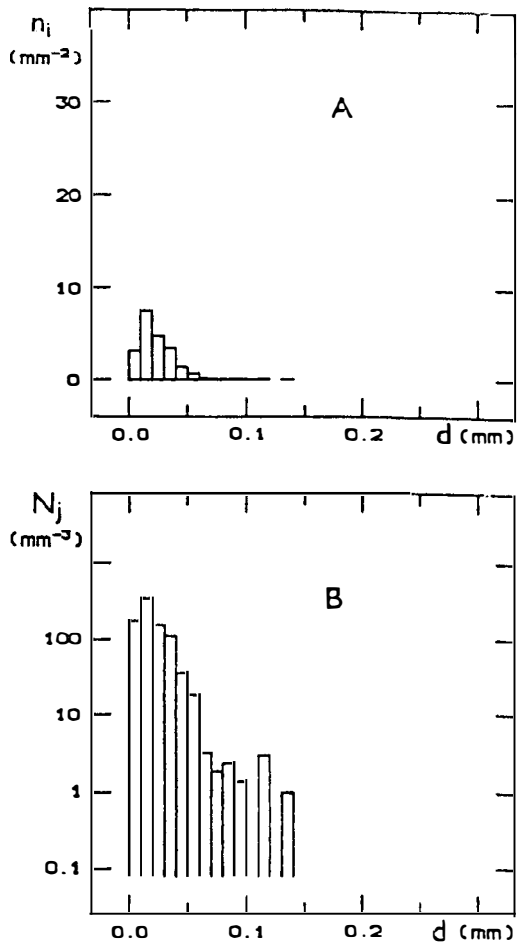

Fig. 4. Size distribution of bubbles, enamel coating No 2. For explanation of symbols see Fig. 3.

Table 1 summarizes the bubble structure parameters determined from stereological calculations. In addition to the quantities defined above, $N_V^{0.1}$ is also given denoting the number of bubbles, the diameter of which exceeds 0.1 mm, per unit volume. Further, t is enamel coating thickness, h distance of the planar section from the original coating surface.

Among the data given in Table I, α and V are of little value from the point of view of protective properties of enamel coatings. On the other hand, V_V and N_V are more important because they characterize a sort of "compactness" of the coating. As a rule, a failure of a protective coating of this type is mostly due to the local occurence of very large bubbles. The tendency of an enamel to develop large bubbles can be seen best from $N_V^{0.1}$ where of course the limit of 0.1 mm is arbitrary. The results show that the above described enamels differ particularly in the values of $N_V^{0.1}$. This is also illustrated by Figs. 3 and 4.

To a good approximation, the properties of bubble systems in both enamel coatings are in agreement with the presumptions of the Scheil-Schwartz-Saltykov method. However, it may happen for particular enamels that this method is not applicable, especially in the case of a high density of very large bubbles where bubble deformation occurs. An example of such an enamel coating is shown in Fig. 5.

A method alternative to the procedure described here is the evaluation of a pair of parallel section planes called "disector". This enables to simplify the mathematical solution presented here, however, more experimental effort is required. This method is not considered in the present paper. For its applications see [9].

CONCLUSION

The above described method complements the conventional set of tests of enamel coatings, such as adherence, porosity, and corrosion tests. The procedure is based on the measurement of bubble sections in

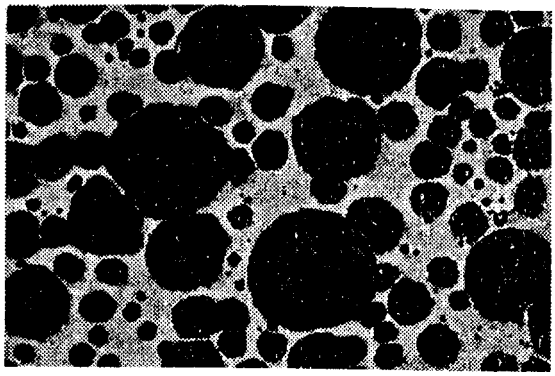

Fig. 5. Optical micrograph of a planar section of a three-frit direct enamel fired under anomalous conditions (12 minutes, hight humidity of furnace atmosphere). For magnification see Fig. 1.

a plane parallel to the coating surface and on a stereological evaluation of the results. The method yields quantitative data characterizing thoroughly the bubble structure of enamel coatings.

References

[1] Deriemont Y.: Sprechsaal für Keramik, Glas, Email, Silikate *98*, 511 (1965).

[2] White D.: Mitteilungen VDEfa *30*, [3] 25 (1982).

[3] Hoens M.F.A.: Mitteilungen VDEfa *30*, [4] 37 (1982).

[4] Joseph W.A.: The Vitreous Enameller *39*, [1] 21 (1988).

[5] Voleník K., Seberíni M., Cirák J.: Izv. An Latv. SSR, Chem Series, Riga, No 3, 294 (1977).

[6] Stoyan D., Kendall W.S., Mecke J.: *Stochastic Geometry and Its Applications*, Akademie-Verlag, Berlin 1987.

[7] Saltykov S.A.: *Stereometrische Metallographie*, VEB Deutscher Verlag für Grundstoffindustrie, Leipzig 1974.

[8] Cruz-Orive L.M.: J. Microscopy *131*, 265 (1983).

[9] Beneš V., Starka P., Suchánek V., Slámová M., Voleník K., Bouše V.: Acta Stereol. *11*/Suppl. I, 689 (1992).

Submitted in English by the authors

BUBLINATÁ STRUKTURA SMALTOVÝCH POVLAKŮ A JEJÍ HODNOCENÍ

VIKTOR BENEŠ, VÁCLAV BOUŠE[a], MARGARITA SLÁMOVÁ[b], VLADIMÍR SUCHÁNEK[b], KAREL VOLENÍK[c]

České vysoké učení technické, Fakulta strojní, Katedra matematiky, Karlovo nám. 13, 121 35 Praha 2

[a] *SMALT, spol. s r.o., 267 62 Komárov u Hořovic*

[b] *Výzkumný ústav kovů, Panenské Břežany, 250 70 Odolena Voda*

[c] *Státní výzkumný ústav ochrany materiálu, 190 11 Praha 9 - Běchovice*

Bublinatá struktura smaltových povlaků je významná z hlediska použitelnosti povlaků pro antikorozní ochranu kovů. Rovnoměrně rozložené malé bubliny jsou výhodné, protože omezují výskyt vodíkových vad. Naproti tomu přítomnost velkých bublin o průměru srovnatelném s tloušťkou povlaku je zcela nežádoucí. V místech jejich výskytu totiž snadno vznikou průchozí póry a v agresivnějším prostředí zde dojde k intenzivní korozi kovového materiálu.

Existence bublin je důsledkem vzniku plynů při vypalování smaltu, a to jednak v objemu taveniny smaltu, jednak při povrchové reakci na rozhraní kovu a této taveniny.

Pro hodnocení geometrických vlastností bublinaté struktury smaltových povlaků je možno použít několik metod. Z nich byla zvolena metoda založená na proměření rovinného řezu, vedeného rovnoběžně s povrchem povlaku v předem zvolené hloubce pod povrchem. Pro toto měření je zvlášť vhodná obrazová analýza. Výsledkem měření je distribuce četnosti dvojrozměrných řezů bublin podle jejich průměru. Klasické stereologické metody, např. metoda Scheil-Schwartz-Saltykovova, umožňují rekonstruovat distribuci bublin podle jejich skutečného průměru, a to v objemu smaltu v těsné blízkosti rovinného řezu.

Obrazová analýza rovinného řezu rovnoběžného s povrchem povlaku a Scheil-Schwartz-Saltykova metoda vyhodnocení výsledků měření jsou základem postupu popsaného v této práci. Pro ilustraci použití tohoto postupu jsou uvedeny výsledky, získané u dvou typických smaltových povlaků, které se uplatňují v antikorozní ochraně ocelí.

Mění-li se charakter bublinaté struktury v závislosti na hloubce pod povrchem povlaku, je možno vést rovinných řezů několik a popsaný postup použít pro každý z nich.

Obr. 1. Mikrofotografie rovinného řazu smaltovým povlakem č. 1.

Obr. 2. Mikrofotografie rovinného řezu smaltovým povlakem č. 2. Zvětšení je stejné jako na obr. 1.

Obr. 3. Rozdělení velikosti bublin ve smaltovém povlaku č. 1.
Horní diagram (A): Rozdělení rovinných řezů bublin, stanovené pomocí obrazové analýzy.
Dolní diagram (B): Rozdělení trojrozměrných bublin, odvozené stereologickou metodou z výsledků obrazové analýzy.
n_i ... *počet řezů bublin v i-té velikostní třídě na jednotku plochy,*
N_j ... *počet bublin v j-té velikostní třídě na jednotku objemu,*
α ... *průměr.*

Obr. 4. Rozdělení velikosti bublin ve smaltovém povlaku č. 2. Význam symbolů je stejný jako na obr. 3.

Obr. 5. Mikrofotografie rovinného řezu povlakem třífritového přímého smaltu, vypalovaného při anomálních podmínkách (12 minut, vysoká vlhkost pecní atmosféry). Zvětšení je stejné jako na obr. 1.